Chapter 3

Mechanism of Aggregation Colloid Centers on Surface Ionic Crystals

Utkirjon Sharopov, Bakhtiyar Atabaev,
Ruzmat Djabbarganov and Muzaffar Qurbanov

Additional information is available at the end of the chapter

http://dx.doi.org/10.5772/65517

Abstract

In this chapter, we analyze the kinetics of changes in the intensities of peaks of these aggregate defects as a function of the substrate temperature, as well as study the degradation of these aggregate F centers in order to understand the mechanisms of their formation and transformation to other types of defects, to colloids. The results obtained using methods of total current (TC) spectroscopy and secondary-ion mass spectroscopy (SIMS) under ion bombardment of LiF crystals are analyzed. The temperature dependence of the generation kinetics of F centers and their aggregates in a LiF/Si(1 1 1) thin-film system after irradiation with low-energy (80 eV) electrons was studied by TC spectroscopy. It was shown that, in all cases, low-temperature annealing results in the degradation of the formed centers followed by their coalescence. By SIMS, it is shown that the majority of the products of crystal sputtering contain point defects. A procedure for determining defects in sputtered clusters of ionic crystals is developed.

Keywords: defects, colloids, coalescence, surface, temperature, ion electron bombardment, annealing, ionic crystals.

1. Introduction

It is known that under ionizing irradiation of ionic crystals the anion vacancies at which electrons are trapped are first formed and then the F centers emerge. Their migration over the lattice results in coalescence of point defects and in the formation of large stable aggregates of defects. The migration of defects depends on crystal temperature [1].

In the 1970s, the studies of damage created under electron and ion irradiation were started with the first accelerators [1–5]. For the ions having energy of 1–10 MeV/u the main interaction with diverse solids is Coulomb one, which leads to an extremely high level of electron excitation and makes the processes similar to those in dielectrics and metals [5]. New radiation phenomena in diverse solids such as local phase transitions, volume change, internal stress, etc. [6–8] are due to the high electronic excitation level.

Such features of damage created under fast heavy ion irradiation were observed in LiF and some other ionic crystals (NaCl, NaF, CaF_2). In these crystals the two different zones of damage are induced: in a cylindrical region of the radius of 1–2 nm the defect aggregates are dominating (aggregate damage zone), while in the more extended lateral track region ($r > 2$ nm, track halo), the point defects prevailed [8–10]. It should be noted that the LiF crystals occupy a unique place among the alkali and other ionic crystals owing to their large band gap ($E_g = 14.6$ eV) and corresponding high energy of lattice. As a result, the main radiation defects (F- and V-centers) in the LiF crystals are stable up to 200°C and defect formation in the LiF crystals can be studied for the different values of temperature and within the wide range of excitation energy density.

In alkali halides, the radiation damage was studied in-depth for several decades [1–4, 12–14], which led to the discovery of an exciton mechanism of defect formation. The first V_K-centers and self-trapped excitons were observed in the LiF crystals [4].

The damage induced under irradiation strongly depends on absorbed dose, dose rate, and irradiation [11] temperature. The effect of high dose radiation on the LiF crystals was studied by thermal neutron irradiation. LiF is very sensitive to thermal neutrons due to the reaction of 6Li (n, α)3 T, where 4.78 MeV energy is released. Under irradiation up to the dose of ~1 MGy the single point defects such as F-, F_n-, V-, and V_n-centers ($n \leq 4$) are dominating. For higher dose and higher irradiation temperature ($T \geq 100$–200°C), the single point defects are aggregated and larger aggregates of F- and V-centers are formed. The Li colloids and fluorine molecular clusters (nF_2) are produced within the dose range of 10–100 MGy. The fluorine molecules F_2 are accumulated in the crystal bulk and only a small part of the fluorine molecules goes out of the crystal. For high irradiation dose, the dislocations are also formed and the mechanical stress and swelling effects were observed [12–14].

LiF thin films containing different optically active centers are used in adjustable lasers [15, 16], fiber optics, and molecular spectroscopy. Investigations of the formation kinetics of defects in LiF crystals were performed in Refs. [17–19].

In our study, the formation and aggregation of various point defects, such as F, F_2, F_3, and X centers and colloid centers, were observed upon thermal annealing. The formation and degradation kinetics of aggregate centers and the time-dependent change in the peak intensities of aggregate centers in the total current spectrum upon heating from room temperature to 150°C were also studied.

Upon the irradiation of halide ionic crystals, halogen vacancies, at which electrons are trapped, emerge first to form F centers. It has been shown that F_2^+, Li_4, F_2, F_3, and X centers are produced upon low-dose electron irradiation of LiF films [29].

In the present chapter, we analyze the kinetics of changes in the intensities of peaks of these aggregate defects as a function of the substrate temperature, as well as study the degradation of these aggregate F centers in order to understand the mechanisms of their formation and transformation to other types of defects, to colloids. And the obtained results using methods of SIMS under ion bombardment of LiF crystals as well as procedure for determining defects in sputtered clusters are analyzed. The problem of this paper lies in determining the composition of secondary clusters sputtered from the surface of LiF.

2. Materials and methods

2.1. Total current spectroscopy

The method of TC spectroscopy is some kind of low-energy threshold secondary-ion spectroscopy. For experimental realization of this method a measuring scheme presented in **Figure 1** is necessary. A monokinetic beam of electrons focused with an electronic optical system is directed to the sample surface. In the space between the focused system and plane sample the electrons move in the homogeneous decelerating field and come to the sample with energy defined by the displacement potential. A primary electron current I_1 is defined by a value of the current formed between the electron gun cathode and the sample under study. When the primary electrons interact with a target, some part of the electrons is reflected and creates a current of the secondary electrons I_2 and another one remains in the target and makes a contribution to the current I running through the sample. The current balance is written as follows

$$I_1 = I + I_2 \tag{1}$$

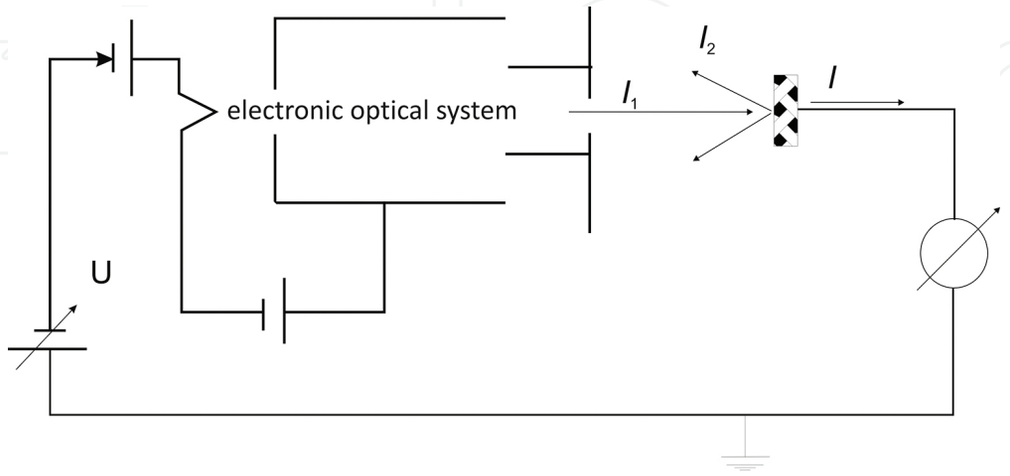

Figure 1. An electric scheme of the total current spectrometer.

Since the relative potentials of the electrostatic system remains the same when the retarding field over the sample changes, the primary electron beam does not lose its focus and the current I_1 remains unchanged in value [20].

Taking that fact into account, it is possible to define the value of the secondary electron current I_2 by measuring the target circuit current I

$$I = I_1 - I_2, \;\; I_1 = \text{const} \tag{2}$$

Applying a small (0.1–0.2 V) sinusoidal voltage of frequency ω to the cathode unit, one can modulate a primary beam in energy and select the first derivative of the sample circuit current with a system of synchronous detection. Then the expression for the current balance can be written in the following form

$$\frac{dI}{dE_p} = \frac{d\left(I_1 - I_2\right)}{dE_p} = -\frac{dI_2}{dE_p} = S\left(E_p\right) \tag{3}$$

Thus, a TC spectrum $S(E_p)$ is a derivative of the target circuit current in energy of incident electrons.

Several works devoted to dielectrics, semiconductors, and metals studied by the TC spectroscopy method showed that the TC spectra have a fine structure that is characteristic of each substance within the low-energy range (0–15 eV) [20, 21]. In Refs. [21, 22], on the basis of the analysis of the energy dependences of elastic and inelastic reflection of electrons from solid surface and taking into account the effect of inelastic interaction on the intensity of elastic reflection, the model describes about TC spectroscopy signal formation, which unambiguously relates the TC spectra structure with the special features of the electronic state density of the valent and free zones of the sample under study.

Colloid formation on the LiF film surface under electron and ion irradiation is described below.

In the high vacuum chamber, an electronic gun is mounted to produce an electron beam with energy $1 < E \leq 80$ eV. Spectrum registration and electron irradiation of film were made with one gun to get information from an irradiated part of the film.

An ion gun was also mounted to irradiate the samples by Cs^+ and Cl^- ions with energy $200 < E \leq 2000$ eV.

An experimental technique for studying the defect and colloid formation on the surface of the growing LiF film according to the following algorithm was developed:

1. Cleaning of the single crystal Si(1 1 1) surface by ion etching and subsequent annealing.
2. Registration of a TC spectrum of the cleaned Si(1 1 1).
3. Deposition of a LiF film on the Si(1 1 1) substrate and further irradiation by electrons with energy $5 < E \leq 80$ eV or Cs^+ ions with energy $200 < E \leq 2000$ eV.

4. TC spectrum registration every 1 min for 30–40 min.

This algorithm was used for different energy irradiation and substrate temperature ($25 \leq T \leq 800°C$).

The advantage of our total current spectrometer is that it provides much more information as compared with others. For example, in Ref. [23] the total current from the LiF films was measured lower than the threshold of electron-stimulated desorption (up to 12 eV). **Figure 2** illustrates the total current spectra of the LiF films of 17 monolayer in thickness. The authors associated the minimums at 3 and 7 eV with deceleration voltage on the surface. Deceleration voltage manifests itself on the surface when the thickness is over 2 monolayers. There are special features near zero energy of the spectrum for thickness of ~10 monolayers.

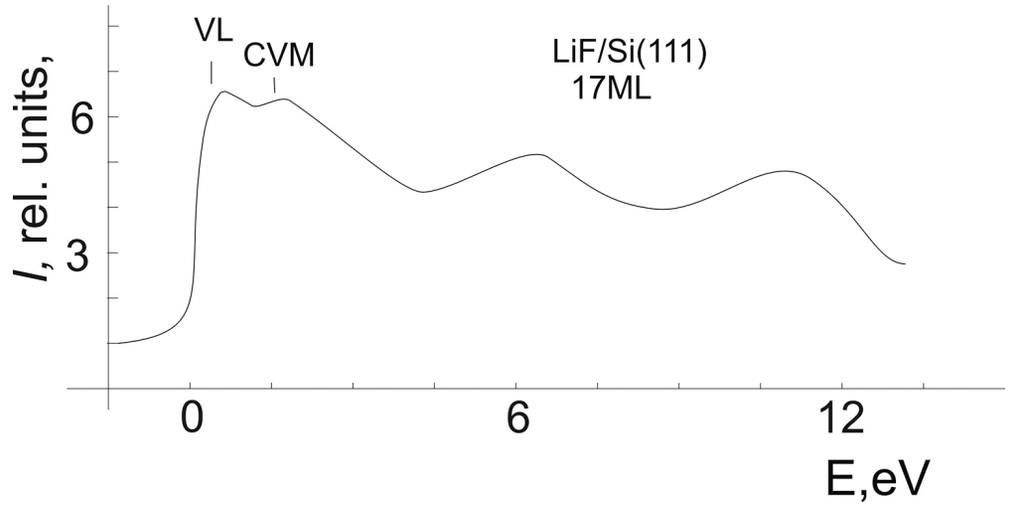

Figure 2. The total current spectrum of the LiF films of 17 monolayers in thickness [23].

From the energy position of the first minimum and decrease in total current, it was established that the electron affinity of the LiF film is 1.2 eV. Also, it was shown that the low-energy part of the spectra demonstrates the basic properties of the density of the electronic states in the conductivity zone. As seen, in this case, the total current has little information, the peaks of the local levels are almost unresolved, and the peak of exciton absorption is not seen since in this technique the current in the sample circuit is not integrated by a registering device. Nevertheless, some of these data can be used for the interpretation of our results.

Also in Refs. [1, 20–23] it is shown that the changes in the intensity of the TC spectra can show defect formation when the whole spectrum of total current is shifted, and also the work function changes, as well as bending of the energy zones takes place, islands are formed, and changes in the surface potential are defined by doubling of the primary peak.

Thus, at present, the TC spectroscopy has become an efficient tool for studying the surface properties of solid. This technique has a whole series of attractive features: it is simple for experimental realization and at the same time can provide much information, it has high surface sensitivity (an order of 10 Åi, and no destruction of the surface takes place under study.

However, for the studies of the surface one should not seek a "better" method but apply, as possible, a combination of the independent methods providing information about the features that manifest themselves more pronouncedly. For example, the characteristics of some atoms of substance are defined by secondary-ion mass-spectrometry, which makes it possible for an elemental analysis of the surface according to the mass spectra. Each technique provides information on some properties of the surface area and only application of several independent techniques allows more exactly and unambiguously solving the study problems in case of correct comparison of the results of independent measurements.

A design of the total current spectrometer allows effective solution of surface cleaning and ordering, and a mass spectrometer can define an elemental composition of a sample under study.

2.2. Vacuum system and experimental setup elements

The measurements were performed with an all-metal chamber having three-stepped oil-free pumping. Preliminary pumping was made by a zeolite pump up to pressure 10^{-3} Torr, then the zeolite pump was blocked with a high-vacuum valve and further pumping was made by an ion pump NORD-160 allowing working pressure of up to 10^{-9} Torr. The experimental setup had additional devices allowing the complex effect on a sample under study with no disturbing of vacuum conditions.

A graduated system of sample heating is necessary for thermal cleaning and measurements within a wide range of temperature. The system consists of a tantalum cylinder with a tungsten spiral of indirect heating inside it. On the end face of the cylinder a sample to be studied is mounted with special holders. A chromel-alumel thermocouple for heating control within the wide range of temperature (20–1500°C) is mounted on the side part of the sample. A special spiral winding was used to prevent the effect of the magnetic field of the heater on the sample under study. To exclude noises of thermoelectron current (when a useful signal was measured in the sample circuit) a positive potential relative to the sample was applied to the heater spiral; that potential did not allow thermoelectrons to go to the sample.

An ion gun operating according to the ionization mechanism was used to clean the sample surface by ion etching. The gun provides the ion current of an order of 1–10 nA and the beam diameter of 0.4 cm. Ion bombardment was performed at an angle of 25° relative to the normal sample surface.

The study objects were thin LiF films (~150 Å50re thin LiF fil 1 1) side of the silicon substrate by thermal evaporation in ultrahigh vacuum. The films of ion crystals were chosen as model objects since they are usually used to develop diverse technologies. LiF is a very simple crystal so the studies with it are very easy. In practice, monocrystals and films of LiF are used to produce high-effective lasers (80% in efficiency).

A LiF evaporator was used to carry on experiments with film systems. The evaporator is a quartz pipe; on its external side a nichrome wire is reeled up. Special glasses located at some distance from the evaporator were used to define the thickness of the deposited layers. After the end of the experiments, these glasses from the chamber were removed, and by measuring the

thickness of the deposited layer (for example, with an interference microscope), one can judge the thickness of the deposited layer on the sample by taking into account the distances of the evaporator-sample and evaporator-glass. Preliminarily, a mode for evaporator operation was selected and the total current spectra were not registered in the process of film growth for different rates of deposition. A film with fewer defects was that spectrum which had less structure, and such conditions occurred at the deposition rate of 3–4 Åf deposition rate fects of film growth for different rates of deposition. A filmsample surface.

2.3. Additional methods

For an element composition of the alkali-haloid crystal surface to be defined by SIMS, comparative studies of the mass composition of the LiF sputtering products were conducted.

It is known that dielectric sputtering under ion bombardment can increase if there are a lot of defects on the target surface. To study the role of defects and colloids in the sputtering processes, some experiments were carried on with a setup described below.

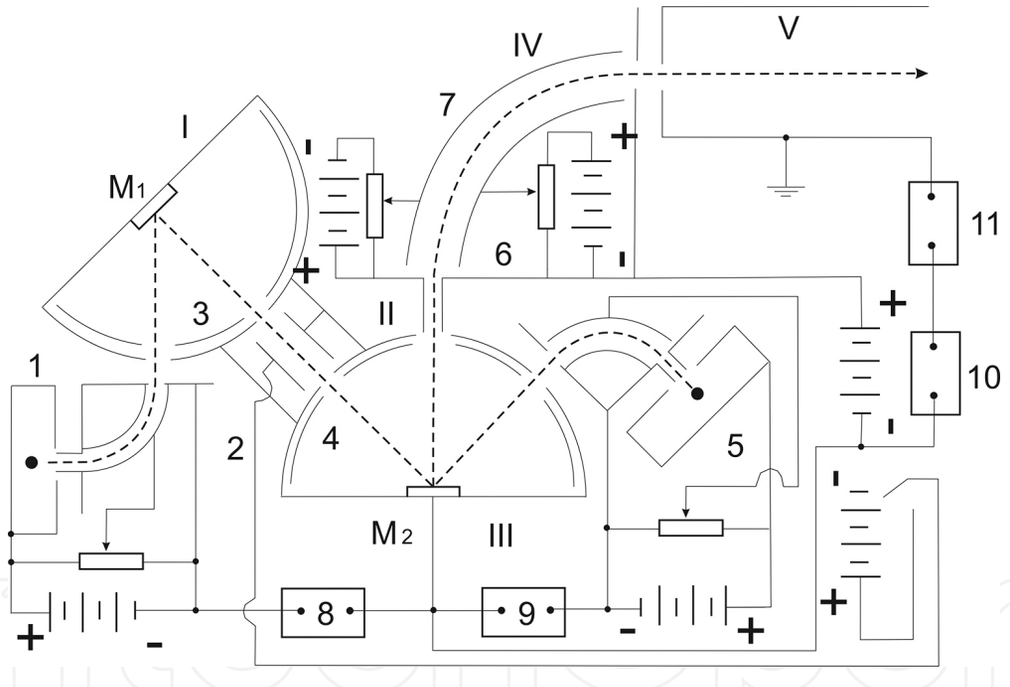

Figure 3. A mass-spectrometer of negative ions.

A setup consisted of the following main parts (**Figure 3**): a sputtering chamber I with an evaporator of primary ions I, a target to be studied M_1, an electrode system to draw out and accelerate the primary ions and to focus them on the target M_1; a cylindrical condenser (in its electrical field a beam of charged particles are separated from neutrals); a chamber to deviate an ion component of sputtering (II); a chamber to ionize the sputtered particles III with a target-ionizer M_2 and a source of primary ions 5; an electrode system to draw out and accelerate the primary ions and to focus them on the target M_2; a cylindrical condenser to separate a beam of charged particles from neutrals; an electrode 6 to draw out secondary negative ions; a 90°

energy analyzer IV and a mass-analyzer V with a mass-spectrometer to analyze the sputtered ions in mass.

The targets to be studied were mounted in the chamber III at the place of the target M_2. In this case, the surface of the studied target M_2 is bombarded by a positive ion beam produced and formed from the ion source 5. Some part of the secondary negative ions sputtered from the target M_2 to the whole front semisphere is taken by a sagged field of the electrode 6 and passing through the cylindrical energy analyzer 7 goes through a gap to the mass-analyzer operating in a mode of energy modulation.

Before entering the mass-analyzer, the negative ions passed through the exit gap of the energy analyzer III and are accelerated by an electric field created by series sources of constant voltage (BC-23) and generator of saw-tooth voltage. The ions that passed through the mass-analyzer enter a receiver of the secondary ions. For rapid involute of the mass spectra, the modulation of voltage accelerating the secondary ions with the help of a generator of saw-tooth pulses was used, now secondary-electron multipliers provide sufficient rate of rapid registration of ion current pulses. Therefore, an electronic multiplier of an open type was chosen as an amplifying device. The output of the secondary-electron multiplier is connected with a vertical input of the electronic oscillograph, and its horizontal involute is synchronized with the modulation of secondary ion energy. For some value of the magnetic field on the oscillograph monitor will be a motionless picture of some area of the mass-spectrogram, its size is defined by the depth of ion energy modulation by the saw-tooth pulse generator. The different regions of the mass spectrum were observed and measured by magnetic field variation.

The mass-spectrometric setup was manufactured from stainless nonmagnetic steel. Vacuum was created by pumps NORD-250 and maintained at a level of ~10^{-8} Torr.

Thus, it is possible to simultaneously make a quantitative analysis of the composition and state of the surface and accurately define how the work function of the sample changes in electron volts.

3. Aggregation colloid centers on surface ionic crystals

Figure 4 shows the kinetics of the TC spectra upon annealing of the LiF film for 120 min at 25°C after irradiation with 80 eV electrons. The TC spectrum exhibits the formation of the peaks of F_2^+, F_2, F_3, and F centers. The peak intensities of the F_2 and F_3 centers increase for 30 min due to the coalescence of F_2^+ and F centers at the surface, after which the peaks disappear slowly due to the formation of X centers in the film.

Upon annealing of the irradiated LiF film at 50°C, the peak intensities of the F_2 and F_3 centers increase for 10 min and disappear after 90 min due to the formation of X centers whose concentration becomes high.

http://dx.doi.org/10.5772/65517

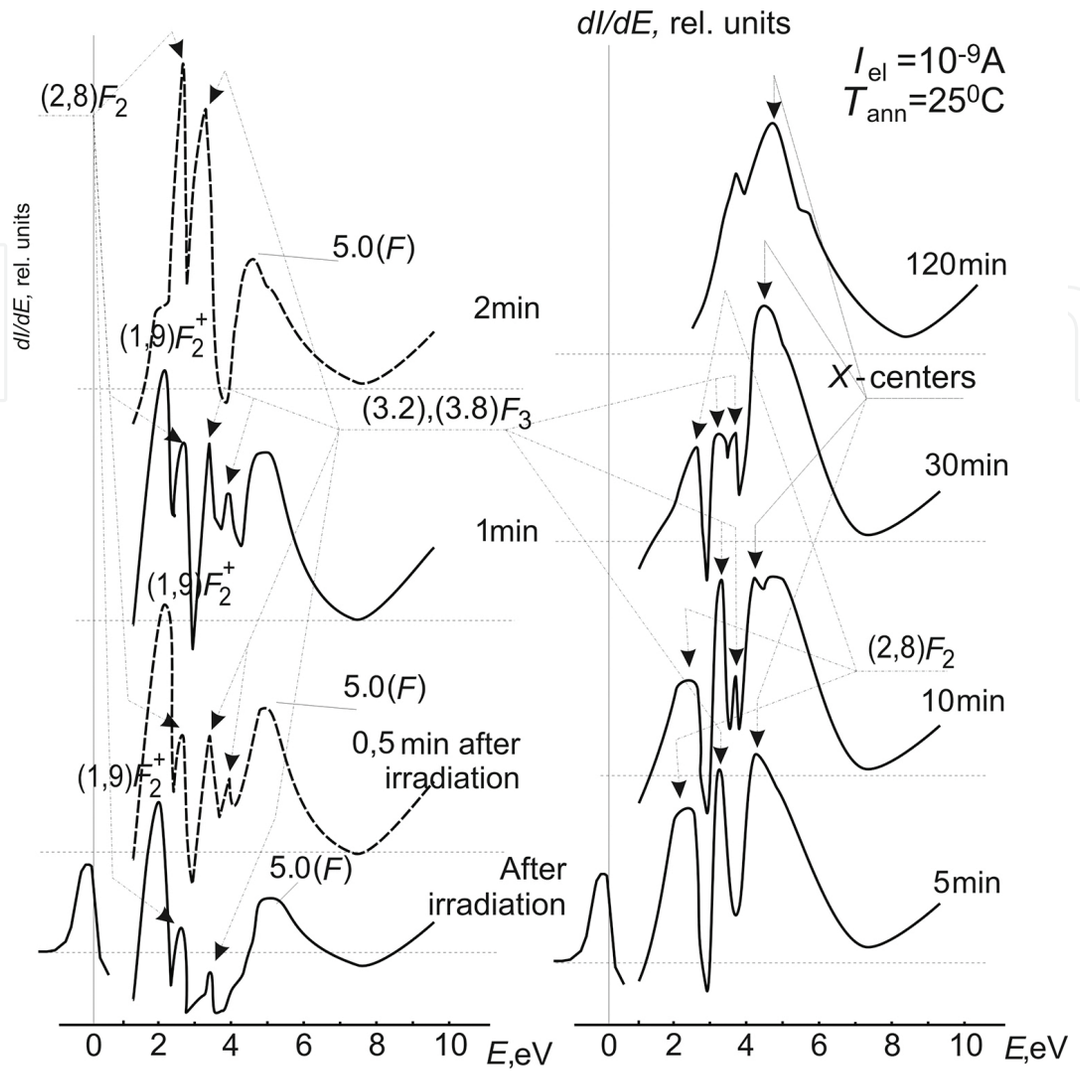

Figure 4. Kinetics of the TC spectra at T = 25°C after irradiation of the LiF film with 80 eV electrons.

When the annealing temperature of the irradiated LiF film is 75°C, the peak intensities of the F_2 and F_3 centers increase for 5 min, the F_2 centers disappear after 15 min, and the F_3 centers disappear after 20 min. A high-intensity peak with an energy of 2 eV appears in the TC spectrum, which belongs to small-size colloid centers. This means that colloid centers can form upon annealing at 75°C, but this process depends on the concentration of the preliminarily generated F centers. Note that 15 min after annealing at 75°C, the peak with an energy of 2.7 eV increases. Since the concentrations of F_2 and F_3 centers decrease to minimum values upon 10-min annealing, the peak with an energy of 2.7 eV belongs only to large colloid centers [18]. Subsequent annealing for 20 min leads to an increase in the concentration of the colloid centers and the appearance of a new peak with an energy of 3.6 eV, which, probably, belongs to halide complexes. Upon intense colloid formation, the concentration of F centers decreases greatly (~70% of F centers coagulate into colloid centers) [18]. The concentration of colloid centers increases due to electron abstraction from F centers. With an increase in the annealing time to ~70–170 min, the intensity of the colloid peak increases significantly.

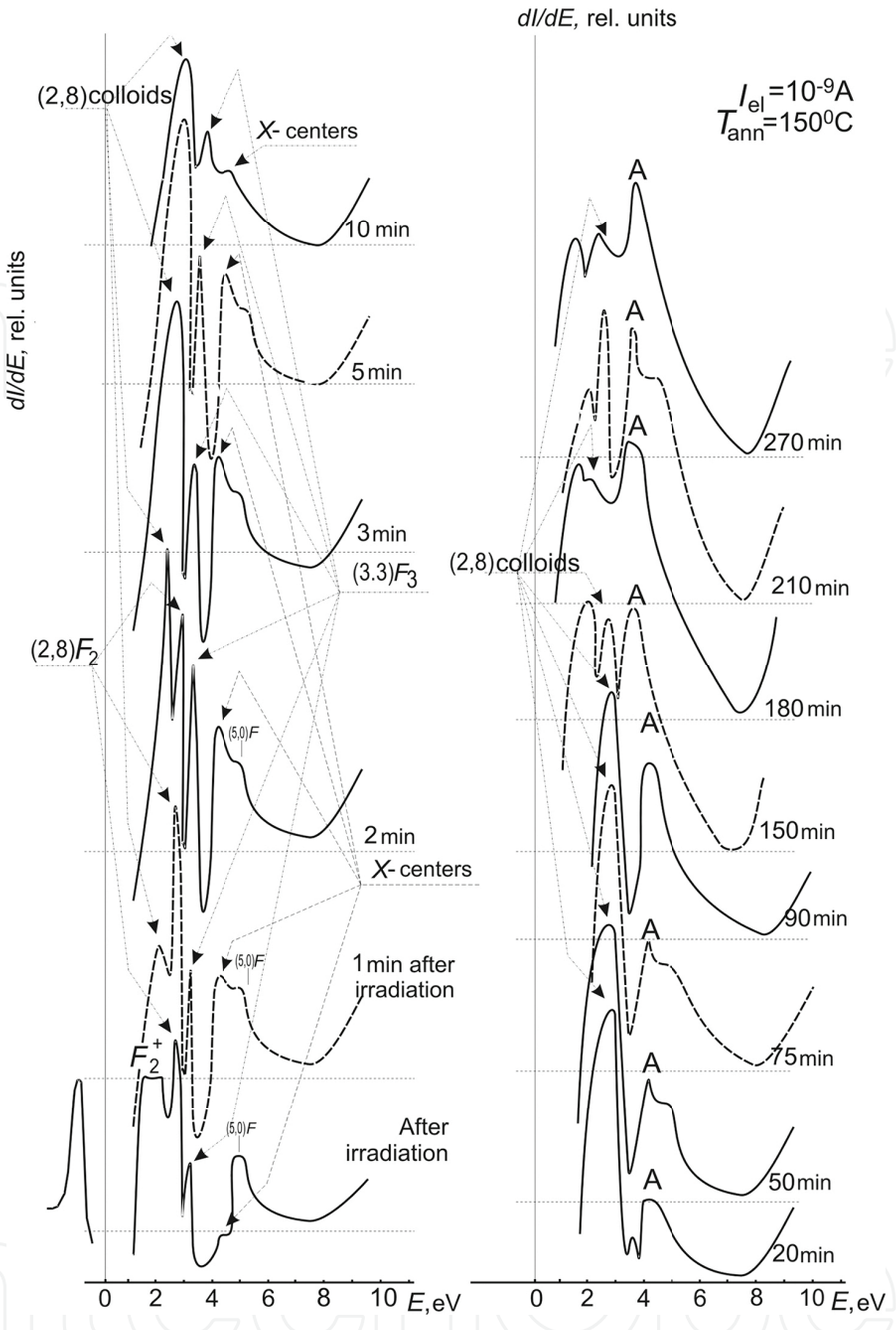

Figure 5. TC spectra at T = 150°C at different time points after irradiation of the LiF film with 80 eV electrons.

After 10-min annealing of the irradiated LiF film at 100°C, the peak intensities of the F_2 and F_3 centers decrease fast and, at the same time, the peak intensities of the X centers (E = 4.5 eV) and colloid centers (E = 2.0 eV) increase greatly. After 20-min annealing, peaks of the large colloids (E = 2.7 eV) and anionic complexes (E = 3.6 eV) appear. Further annealing for 210 min leads to an increase in the concentrations of the colloid centers and anionic complexes.

Annealing of the irradiated LiF film at T = 150°C results in the disappearance of F_2 centers (3 min) and F_3 centers (10 min) (**Figure 5**). Immediately after 1-min annealing, peaks of the X and

http://dx.doi.org/10.5772/65517

colloid centers appear. After 20-min annealing at 150°C, large colloid centers and halide cluster complexes form in the film. TC spectral analysis of the LiF films annealed at different temperatures (25, 50, 75, 100, and 150°C) shows that the F_2 and F_3 centers are in existence for a long time. With an increase in the temperature by 50°C, they exist in the LiF film for just 10–20 min. Annealing of the LiF film at 75°C results in a large accumulation of X centers and colloid centers. With increasing annealing time at different temperatures (75, 100, and 150°C), anionic complexes form along with the colloid centers, presumably, due to the migration of cations to the surface upon metallization. Lattice deformation results in the accumulation of halide atoms and H centers and the formation of anionic complexes.

Figure 6 shows the degradation kinetics of F_2 centers at different temperatures after deposition of the LiF film (F_2 centers form due to the localization of two electrons at two anion vacancies). The model of an F_2 center has been described in Ref. [10]. The point symmetry of F_2 centers is identical in all crystals; this means that an F_2 center has only one absorption band in the spectrum (2.76 eV). It follows from the analysis of **Figure 6** that low-temperature (50–150°C) annealing leads to an increase in the peak intensity of the F_2 centers in the TC spectrum due to the migration and coalescence of F centers and their components from the bulk to the surface. A sharp decrease in the F_2 center peak at 75–150°C indicates the formation of colloid and X centers at the surface. Room-temperature annealing leads to an increase in the peak intensity of F_2 centers due to the coalescence of F centers and their components (vacancies, F_2^+, and F). With increasing temperature to 50°C, the kinetics of the peak intensity of F_2 centers increases two-fold. With a further increase in the annealing temperature to 75 and 100°C, the peak intensity of the F_2 centers decreases appreciably, but their survival time remains unchanged. At 150°C, the peak intensity of the F_2 center increases quickly and then drops to zero in 3 min. As seen, the concentration of F_2 centers always increases upon annealing. The increase in the concentration of a certain defect type always results in the degradation of this defect due to the formation of another large defect upon their fusion with one another. Therefore, the concentration of F_2 centers drops to zero after several minutes. It is seen that the degradation of F_2 centers occurs faster when the annealing temperature is higher.

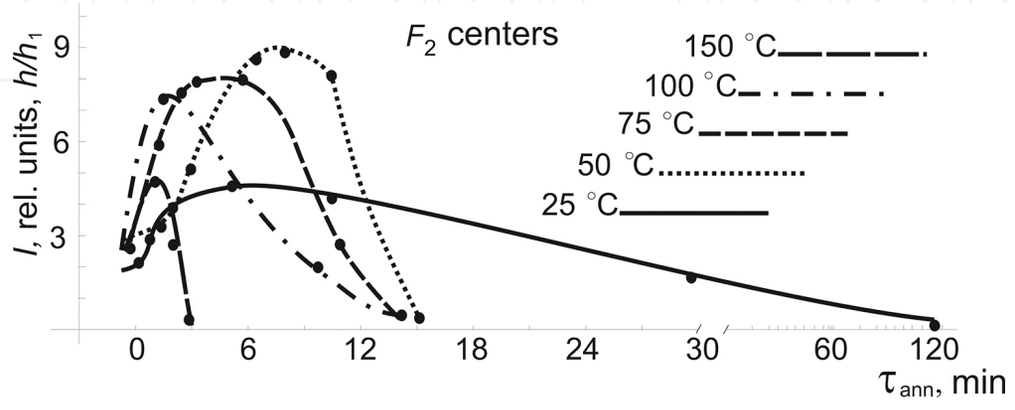

Figure 6. Kinetics of the peak intensity of F_2 centers at different annealing temperatures of the LiF film.

Figure 7 shows the kinetics of the peak intensity of F_3 centers at an annealing temperature of 25–150°C. It is seen that the degradation kinetics of F_3 centers differs from that of F_2 centers: at low temperatures, F_3 centers exist longer. An F_3 center corresponds to three F centers, which can be represented as three anionic vacancies forming an equilateral triangle in the (1 1 1) plane of the LiF lattice and as three electrons moving in the positive field of vacancies. Particularly, an F_3 center has several absorption bands in alkali halide crystals and there are two such bands in LiF (E = 3.3 and 3.9 eV) [10].

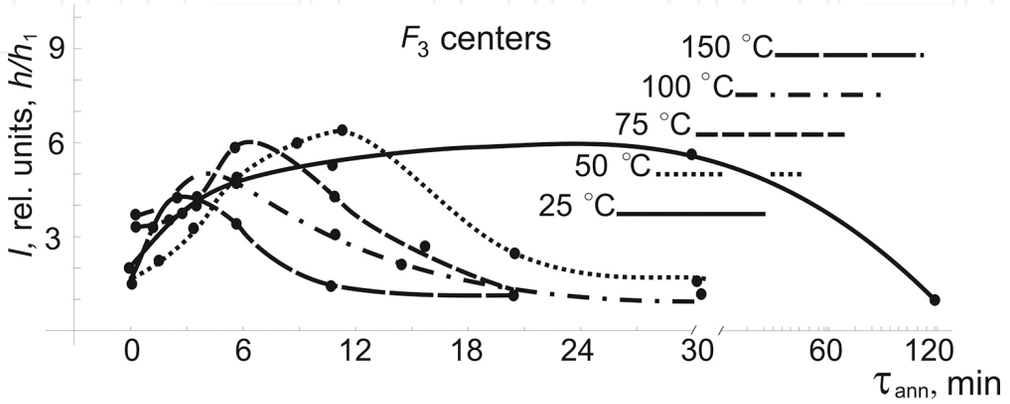

Figure 7. Kinetics of the peak intensity of F_3 centers at different annealing temperatures of the LiF film.

With increasing temperature, the concentration of F_3 centers increases fast and then decreases to zero. One can note that the higher the annealing temperature, the faster the increase in the peak intensity of these aggregate centers. This can be caused by the fact that at high annealing temperatures the coagulation and diffusion of large aggregate centers proceeds in less time. The data in **Figure 4** suggest that the peak intensity of F_3 centers at T = 25°C increases slightly and drops to zero after 2 h of observation due to the formation of the X centers. At 50, 75, and 100°C, the concentration of F_3 centers increases by four-, three-, and two-fold, respectively. Such an increase can be explained by the fact that annealing of the film accelerates the migration and diffusion of color centers from the bulk to the near-surface layer, but with increasing annealing temperature, the formation of X centers and colloid centers proceeds faster, which leads to a decrease in the concentration of aggregate centers. With a further increase in the temperature, the surface is enriched with colloid centers and X centers, which prevents growth in the peak intensity of F_3 centers due to their coalescence into large aggregate centers.

As seen, all aggregate centers coalesce after thermal annealing to form large centers, such as colloid and X centers, which are more stable than other aggregate centers. In our experiments, the X center peak appears in the TC spectrum at an energy of 4.5 eV. Their creation requires a corresponding dose rate and temperature [22]. **Figure 8** shows the kinetics of the peak intensity of the X centers at different substrate temperatures after deposition of the LiF film. It is seen that the X centers do not degrade and coalesce into colloid centers at low temperatures. At an annealing temperature of 50°C, the peak intensity of the X centers decreases appreciably, but at this temperature, the X centers also do not coalesce into colloid centers. With increasing temperature to 75°C, the X centers in the LiF film degrade in 30 min. Only at T = 150°C does

http://dx.doi.org/10.5772/65517

the peak intensity of the X centers decrease quickly (in 15 min). The concentration of X centers depends on the concentration of precreated F centers and their aggregates. The increase in annealing temperature results in their degradation and transition to the state of a colloid center. The increase in the concentration of F centers results in the accumulation of cations surrounded by F centers. After trapping a sufficient amount of electrons, such a center stabilizes into the colloid aggregate (negatively charged center), which acquires a structure untypical of a macroscopic metal. With increasing size of such particles, aggregates with a true metallic bond form [17, 22]. Colloid centers emerge at high radiation doses, but, for their formation, thermal annealing can also be used, wherein conditions that accelerate the coalescence and migration of F centers can be created.

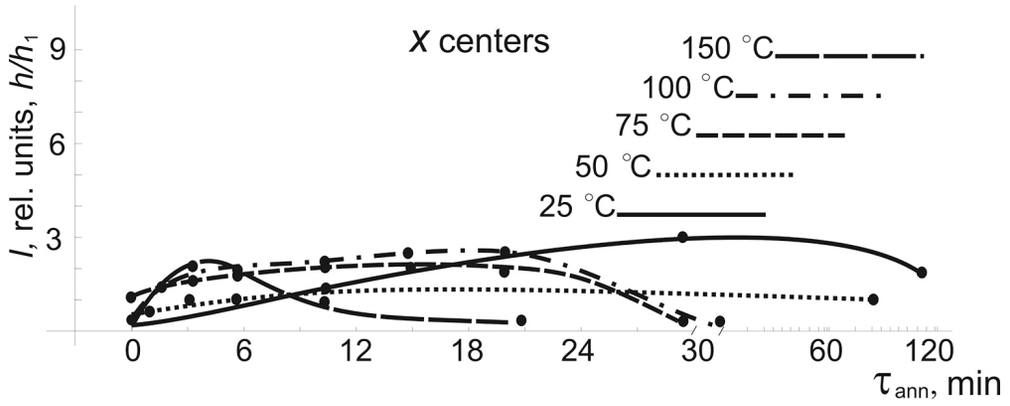

Figure 8. Kinetics of the peak intensity of X centers at different annealing temperatures of the LiF film.

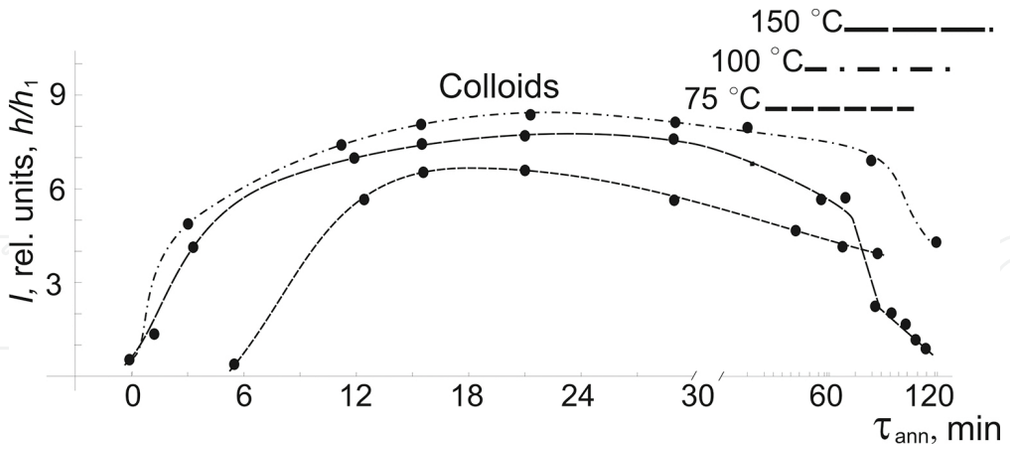

Figure 9. Time change in the peak intensity of colloid centers at different annealing temperatures of the LiF film.

Figure 9 shows the time dependence of the peak intensity of colloid centers upon annealing of the LiF film after deposition. It is seen that with increasing temperature, the formation time of colloid centers decreases. At room temperature, the migration of F centers proceeds slower than at high temperatures. At 25–50°C, no colloid centers form and, with increasing temperature to 75°C, they emerge even 5 min after annealing. At T = 100°C, the colloid centers form

after 1 min. At T = 150°C, the concentration of colloid centers increases fast, and after 1-h annealing, begins decreasing due to evaporation of the colloid center components. At higher temperatures, evaporation occurs faster.

4. Procedure for determining defects in sputtered clusters of ionic crystals

Secondary ions, which are recorded in the spectra of SIMS, can be products of recombination [24, 25] or direct emission [26] from the lattice and can also be produced as a result of defect formation on the crystal surface [27–30]. The authors of almost all papers concerning sputtering have asserted that defects stimulate the formation of secondary clusters [24, 27–37]. Defect formation during crystal sputtering was considered in Refs. [31–34] as a result of the formation of self-localized excitons such as electron-hole pairs, which is accompanied by excitation of the valence band. In some insulator materials (alkali-halide crystals, SiO_2, Al_2O_3), defects can be formed under bombardment with electrons (electron-stimulated desorption) and photons (photon-stimulated desorption) [35–37]. In this case, as a result of the decay of self-localized excitons, neutralized anions (halides in alkali-halide crystals and oxygen in SiO_2 and Al_2O_3) are desorbed and cations are neutralized in the case of alkali-halide crystals, which lead to desorption in the case of small transfer of the bombarding ion momentum.

An analysis of published papers indicates that, at present, there is no procedure for recording point defects in secondary clusters neither in terms of experiment nor theory. Upon collision between primary particles and a crystal, defects are formed on its surface; they not only stimulate sputtering, but also can be emitted together with secondary ions.

Bombardment of the LiF crystals with 0.6 keV Cs^+ ions led to the appearance of a series of peaks, which corresponds to H_N, F_2^-, and F centers, in the TC spectra (**Figure 10**). (An F center is an anion vacancy with a captured electron [22], and H_N centers are attributed to interstitial crystal defects and appear in the absorption energy region of 1.7 eV.) In our case, H_N centers are formed in the target during Cs-ion implantation. These centers are very stable and did not disappear upon annealing up to a temperature of 200°C. Their concentration increased with increasing dose. An increase in the dose of bombarding ions up to 4.5×10^{13} ion/cm^2 led to an increase in the F, F_2, F_3, and F_4 peak intensities (**Figure 10**, curve 3) and also to the appearance of a peak of X centers, which formed in the case of cation accumulation around the F centers. The larger the concentration of F centers, the more stable the X centers [22].

The change in the position of the primary peak indicates the presence of positive charge on the sample surface [20]. A further increase in dose of up to 9×10^{13} ion/cm^2 led to a decrease in the intensities of all peaks (**Figure 10**, curve 5), which indicates surface amorphization. In this case, a wide peak at an energy of 3.5–4.1 eV appeared in the TC spectrum; it can be identified as a complex of anions (V_k centers) in LiF. This can mean that, under Cs^+-ion bombardment, aggregates of F centers lost weakly bound electrons during colloid formation, which affected the formation of anion complexes because of a decrease in the concentration of F centers and their aggregates. As a result, the concentration of colloids and halide complexes in LiF increased. A further increase in the dose of Cs ions up to 10^{14} ion/cm^2 led to the formation of

http://dx.doi.org/10.5772/65517

metal islands on the substrate surface. Based on the data in **Figure 10**, we can state that, if anion complexes are formed under bombardment, then the lattice contains interstitial F atoms, which are recorded during sputtering in the form of positive and negative F_2, F_3, and F_4 ions. If colloid centers are formed, then positive and negative ions of the Li_2, Li_3, and Li_4 types should be recorded. This can be verified using SIMS.

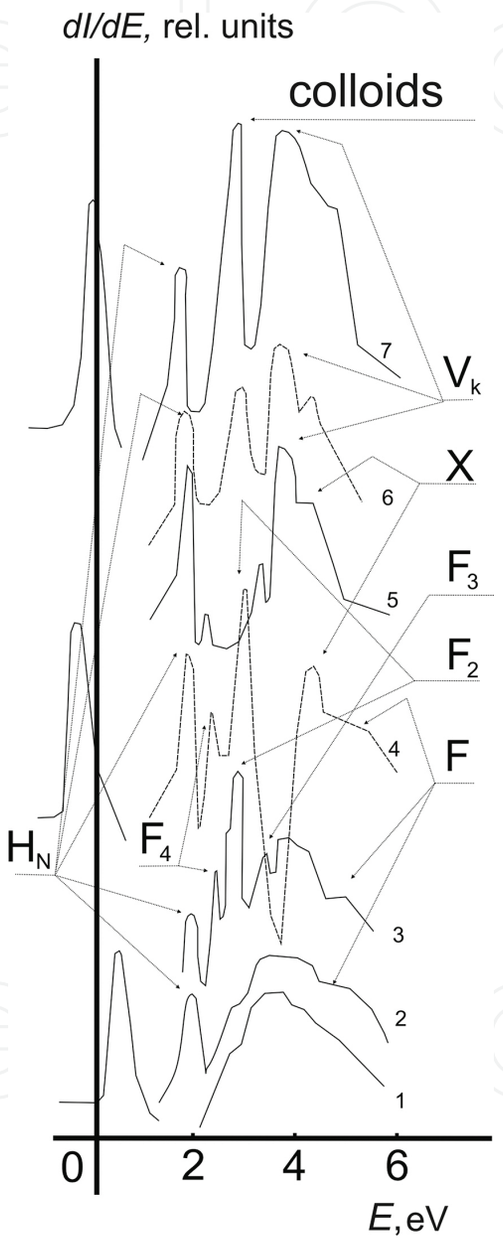

Figure 10. Change in the spectrum of the total current from the LiF crystal under Cs^+ bombardment. Cs^+ doses (ion/cm^2): (1) 0, (2) 2×10^{13}, (3) 4.5×10^{13}, (4) 5.4×10^{13}, (5) 9×10^{13}, (6) 1.4×10^{13}, and (7) 10^{14}.

Figure 11 shows data on secondary ion emission from the LiF crystal under bombardment with positive Ar^+ ions. When measuring the yield of positive ions from the cleaned target surface in this case, it was established that the SIMS spectrum of sputtered particles consists

mainly of Li^+ cations, F^- anions, and molecular Li^+, $Li^+(LiF)n$ ions, where n = 1–5. Li^+ cations in the complex with neutral clusters $(LiF)n$ of the compositions $Li^+(LiF)$, $Li^+(LiF)_2$, and so on, dominate in the SIMS spectra of positive ions.

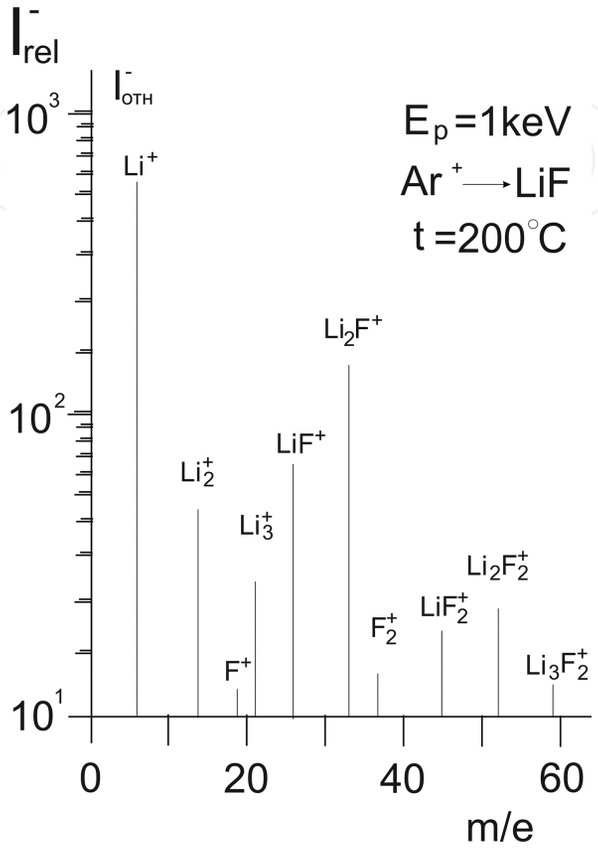

Figure 11. SIMS spectra of positive secondary-ion emission from the LiF crystal under Ar^+ ion bombardment.

Secondary particles			
Li^+	Ion from the lattice	Li^-	Ion from the colloid center
Li_2^+	Ion from the colloid center	F^-	Ion from the lattice
Li_3^+	Ion from the colloid center	F_2^-	F ion with a *H* center
F^+	Ion from the lattice	F_3^-	F ion with a *H* center
F_2^+	*H* center	LiF^-	F ion with a *H* center
LiF^+	Li ion with a *H* center	LiF_2^-	Ion from the lattice
LiF_2^+	Li ion with a *H* center	Li_2F^-	Cluster from the colloid center
$Li_2F_2^+$	Cluster with a *H* center	LiF_3^-	Cluster with a *H* center
$Li_3F_2^+$	Cluster from the lattice	LiF_4^-	Cluster with a *H* center

Table 1. Positive and negative secondary ions that can be sputtered from the LiF crystal surface together with possible defects.

http://dx.doi.org/10.5772/65517

Table 1 shows positive secondary ions emitted from the LiF crystal, which can be sputtered from a surface with possible defects. Analysis of the positive secondary clusters showed that every three clusters in five contain defects formed on the ion crystal surface during transfer of the energy of the bombarding ion.

For example, the secondary Li^+ ion could be knocked out from the colloid center, because two Li atoms cannot be located at neighboring lattice sites. The secondary $Li_2F_2^+$ cluster consists of separate atoms in the form (LiF)(F)Li^+:(LiF), which is a part of the lattice; Li^+ can also be a part of the lattice, but neutral F does not bind with any of the constituents of this cluster (**Figure 12a**).

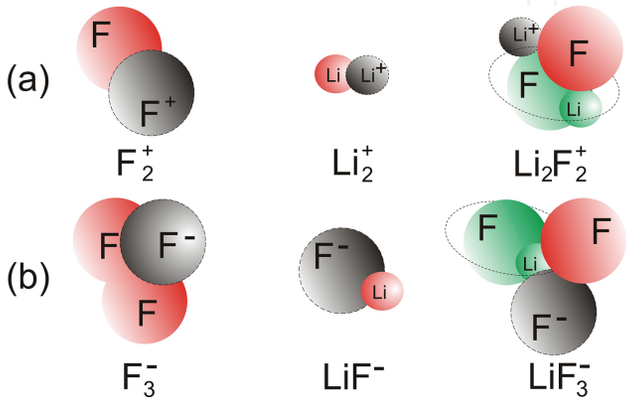

Figure 12. Possible variants of defect structures and orientations in secondary clusters produced under ion bombardment of the LiF crystal: (a) positive and (b) negative clusters.

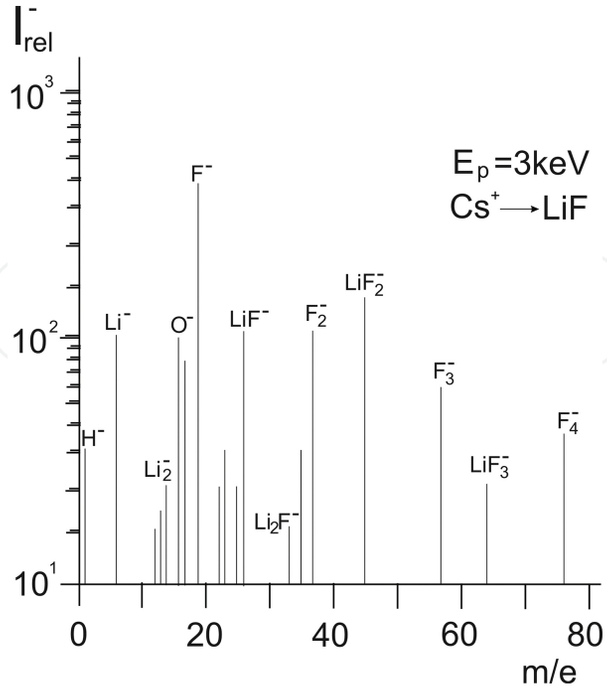

Figure 13. SIMS spectra of negative secondary ion emission from the LiF crystal under Cs^+-ion bombardment.

The study of secondary ion emission from an uncleaned LiF crystal under Cs^+-ion bombardment showed that negative ions F ~ (n = 1–4), Li_m (m = 1–3), $(Li_mF_n)^-$, where n = 1–4, m = 1, 2, $(LiO)^-$, $(CF)^-$, $(FO)^-$, and $(LiFO)^-$ are contained in the SIMS spectrum of LiF sputtering products. The yields of heavy ions observed in the SIMS spectra can be associated with an increased content of defect structures on the uncleaned surface. In this case, the rate of defect formation under bombardment and the intensity of surface-layer sputtering are very large.

Figure 13 shows the SIMS spectrum of LiF crystal sputtering products after long-duration cleaning with Cs^+ ions. Because fluorine is an electronegative element, the number of negative ions is larger, which is seen from this spectrum.

The table contains negative secondary ions from the LiF crystal, which can form on the surface during defect formation. It can be seen that every four negatively charged clusters in five contain surface defects produced by bombardment of the ionic crystal and attached to them. For example, the secondary F_2^-, ion was, probably, ejected together with the H center, because two F atoms cannot be located at neighboring lattice sites, and, especially as one of them is neutral.

The secondary LiF_3^- cluster consists of separate atoms in the form $(LiF)(F)F^-$, where (LiF) is a part of the lattice, F^- can also be a part of the lattice, but neutral fluorine does not bind with any of the components of this cluster. The likely structure of these ions is shown in **Figure 12(b)**. Here, the secondary ion is $F_3^- = F^-(FF)$. This means that the cluster F_3^- consists of one F^- ion and two interstitial defects (FF). The cluster F_3^- cannot be a crystal-lattice product, because only F^- and Li^+ ions together can form a part of the ionic crystal (**Figure 12b**, ellipse). In all other cases, secondary negative clusters are formed by interstitial, colloid, and aggregate V_k centers. Thus, it is very probable that the main part of the charged products of LiF-ionic-crystal sputtering consist of point defects.

It was established that, at low temperatures of alkali-halide crystals, the main sputtering mechanism includes elastic collisions between the impinging primary particles and the target components and, as the temperature increases, the increase in sputtering can be associated with the generation of defects in the form of F—H pairs in the surface layer [22]. The F—H pair is an anion vacancy with a captured electron (the F center) and an interstitial halide atom (the H center), which are formed under bombardment with charged particles. Approximately 60 eV is spent on the formation of an F—H pair in LiF crystals. The formation of primary F—H pairs is most important for sputtering. In accordance with Refs. [22, 31, 35], the increase in the sputtering of alkali-halide crystals with increasing temperature was related to the diffusion of these defects to the surface, which results in the neutralization of surface cations and anions. The latter lacking bonds can participate in both sputtering and evaporation of the target material. If the fact that, in the case of the given energy E_0, the ranges of heavy Cs^+ ions in the LiF crystal, which are smaller than that of Ar^+ ions, is taken into account, then the effectiveness of the formation of defects (including F—H pairs in the surface layer) is relatively high. In this case, defect diffusion to the surface is facilitated as a result of an increase in the bombarded-target temperature, which was observed in our experiment (**Figure 11**). The secondary-emission characteristics of insulators of the alkali-halide type are usually changed if a charge is produced on the surface bombarded with ions. Surface charging causes the deterioration of

beam focusing, a shift of the energy spectrum of secondary ions, a decrease in its intensity, and the migration of primary ions over the sample surface. The effect can be enhanced as the density of the bombarding-ion beam increases. To remove the charge, a thermal method is traditionally used. Our studies showed (**Figure 11**) that, if beams of Ar^+ ions with an intensity of 10^{-9} A are used, the charge on the surface will be suppressed in the temperature range of 100 to 100–180°C, where the LiF crystal does not undergo evaporation.

At low bombardment doses, the concentrations of vacancies and implanted defects in crystals are usually small. Therefore, an insignificant number of cluster ions are observed in the case of LiF-surface bombardment with ions with small energies (300 eV) and at low doses. The increase in the yield of cluster ions with increasing primary-ion energy and dose is due to the fact that, in this case, the number of vacancies and implanted defects increases considerably and more and more F and Li ions penetrate into positions of implanted defects or vacancies near other Li and F ions, which facilitates the process of cluster formation. Thus, as the dose, the bombardment energy, and the temperature increase, a large number of aggregate defects, colloids, and neutralized anion complexes form and are sputtered from the surface together with the clusters.

Analysis of the SIMS spectra of ionic crystals showed that neutralized atoms in the compositions of secondary ions can mainly indicate the presence of defects in them. This procedure can now be used only for ionic crystals. It follows from the foregoing that defects formed on the surfaces of alkali-halide crystals stimulate the sputtering process and are emitted from the surface together with secondary ions in this case.

5. Conclusion

In all cases, low-temperature annealing of the LiF/Si(1 1 1) film results in the degradation of the formed centers followed by their coalescence into large aggregates. Long-term annealing results in evaporation of the halogen atoms and, after electron trapping by cations at the film surface, the formation of colloid centers begins followed by metallization of the surface. The optimal temperatures for the formation of colloid centers on the surface are 75–150°C: at these temperatures, they remain in the film for 5 h. At high temperature (75–500°C), long-term annealing of the LiF film, along with colloid centers (E = 2.7 eV), anionic complexes (E = 3.6 eV) form on the surface.

Point defects formed on the surface of a LiF crystal under ion bombardment not only stimulate the process of cluster formation, but also can be ejected from the surface together with secondary ions. Colloids stimulate Li-cluster sputtering and aggregates of V_k centers, whose compositions contain H centers, increase the yield of F cluster ions. Analysis of the SIMS spectra of LiF ionic crystals subjected to ion bombardment showed that the neutralized atoms in the compositions of secondary ions can mainly indicate the existence of defects in the sputtered clusters. The developed procedure can be useful for the development of theoretical models of structures and orientations of defects in clusters, which are products of the ion bombardment of alkali-halide crystals.

Author details

Utkirjon Sharopov*, Bakhtiyar Atabaev, Ruzmat Djabbarganov and Muzaffar Qurbanov

*Address all correspondence to: utkirstar@gmail.com

Tashkent State Technical University, Tashkent, Uzbekistan

References

[1] Hersch H.H. Proposed excitonic mehcanism of colour center formation in alkali halides. Phys. Rev. 1966;148(2):928–932. DOI:10.1103/PhysRev.148.928

[2] Itoh N. Formation of lattice defects by ionizing radiation in alkali halides. J. Phys. Colloques. 1976;37(C7-27-C7):37. DOI: 10.1051/jphyscol:1976703

[3] Itoh N. Bond scission induced by electronic excitation in solids: A tool for nanomanipulation. Nucl. Instr. Meth. B. 1997;(122) :405.

[4] Lushchik C.B. Physics of radiation effects in crystals. R.A. Johnson and A.N. Orlov (ed.). Elsevier, Amsterdam. 1986; pp. 473–525.

[5] Vetter J., Scholz R., Angert N. Investigation of latent tracks from heavy ions in GeS crystals by high resolution TEM. Nucl. Instr. Meth. B. 1994;(91):129. DOI: 10.1016/0168-583X(94)96202-2

[6] Wiesner J., Traeholt C., Wen J.-G., Zandenbergen H.W., Wirth G., Fuess H. HREM of heavy ion induced defects in superconducting Bi-2212 thin films in relation to their effect on Jc. Physica C. 1996;(268):161.

[7] Schwartz K. Electronic excitations and defect creation in LiF crystals. Nucl. Instr. Meth. B. 1996;(107):128. DOI: 10.1016/0168-583X(95)00846-2

[8] Schwartz K., Geiss O. Chemical etching of ion tracks in LiF crystals Journal of applied physics. J. Appl. Phys. 1998;83(7):3560–3564. DOI: 10.1063/1.366572

[9] Schwartz K., Trautmann C., Steckenreiter T., Geiss O. Damage and track morphology in LiF crystals irradiated with GeV ions. Phys. Rev. 1998;58(17):11232 . DOI: 11232 10.1103/PhysRevB.58.11232

[10] Agullo-Lopez F., Catlow C.R.A., Townsend P.D. Point defects in materials. Academic Press (ed.). London: Academic Press; 1988. 125 p .

[11] Gilman J.J., Johnston W.G. Dislocations, point-defect clusters, and cavities in neutron irradiated LiF crystals. J. Appl. Phys. 1958;(29):877. DOI: 10.1063/1.1723322

[12] Peisl H., Balzer R., Waidelich W. Schottky and Frenkel disorder in KCl with color centers. Phys. Rev. Lett. 1966;(17):1129. DOI: 10.1103/PhysRevLett.17.1129

[13] Montereali R.M. Miniaturized structures based on color centers in lithium fluoride: Optical properties and applications. Rad. Eff. Defects Solids. 2002;(157):545. DOI: 10.1080/10420150215835

[14] Weber M.J. (ed.). Handbook of Lasers. Washington, DC: CRC Press; 2001. 235 p.

[15] Scaglione S., Montereali R.M., Mussi V., Nichelatti E. F-color centers and lithium nanoclusters in ionbeam assisted LiF thin films. Optoelectron. Adv. Mater. 2005;(7):207.

[16] Roberts J.G., van Hove M.A., Somorjai G.A. Surface structural analysis of LiF(1 0 0) thin films grown on Pt(1 1 1). Surf. Sci. 2002;(518):49. .

[17] Ostrovskii I., Ostrovskaya N., Korotchenkov O. Radiation defects manipulation by ultrasound in ionic crystals. IEEE Trans. Nucl. Sci. 2005;52(6):3068–3073. DOI: 10.1109/TNS.2005.861476

[18] Komolov S.A. Integral secondary electron spectroscopy of surface. Leningr. Gos. Univ. (ed.). Leningrad: Leningr. Gos. Univ.; 1986. 146 p.

[19] Henrich V.E. Fast, accurate secondary-electron yield measurements at low primary energies. Rew. Sci. Instr. 1973;44:456–462. DOI: 10.1063/1.1686155

[20] Komolov S.A., Chadderton L.T. Interaction of slow electrons with surface: Desorbtion and adsorption of gas on (1 0 0) vanadium. Rad. Eff. 1976;31:1–6.

[21] Alidzanov E.K., Atabaev B.G., Gaipov C.G., et al. Target current spectroscopy of the alkali halides KCl, CsCl and KBr. Thin Solid Films. 1994;270:268 .

[22] Shvarts K.K., Ekmanis Y.A. Radiation Processes and Radiation Hardening of Dielectric Materials. Riga: Zinatne [in Russian]; 1989. 168 p.

[23] Golek F., Sobolewski W.J. Transmission of low-energy electrons through polycrystalline LiF films. Phys. Status Solidi. 1999;(1):210–211.

[24] Sigmund P. Fundamental processes in sputtering of atoms and molecules. Mat. Fys. Medd. 1993;(43):1.

[25] Dzhemilev N.K. Statistical mechanism of the formation of the energy spectra of sputtered molecular clusters. Surf. Invest. 2012;(6):654.

[26] Wittmaack K. On the mechanism of cluster emission in sputtering. Phys. Lett. 1979;(69):322.

[27] Seifert N., Yan Q., Barnes A.V., et al. Beam interactions with materials and atoms. Nucl. Instrum. Methods Phys. Res. 1995;(101):131.

[28] Reichling M. Electron stimulated desorption from CaF_2: Penetration depth of electrons and sample charging. Nucl. Instr. Meth. Phys. Res. 1995;101:118.

[29] Atabaev B.G., Gaipov S., Sharopov U.B. Investigation of point defects and their clusters formation on a growing film LiF/Si (1 1 1) surface under electrons irradiation. Poverkhnost. 2007;(10):52.

[30] Sharopov U.B., Atabaev B.G., Djabbarganov R., Kurbanov M.K. Kinetics of aggregations of F2, F3, X, and colloid centers in LiF/Si(1 1 1) films upon low-temperature annealing. J. Surf. Invest. X-ray, Synchrotron Neutron Tech. 2013;7:195. DOI: 10.1134/S1027451012120117

[31] Neidhart T., Pichler F., Aumayr F., et al. Potential sputtering of lithium fluoride by slow multicharged ions. Phys. Rev. Lett. 1995;(74):5280. DOI: 10.1103/PhysRevLett.74.5280

[32] Sporn M., Libiseller G., Neidhart T., et al. Potential sputtering of clean SiO2 by slow highly charged ions. Phys. Rev. Lett. 1997;945. DOI: 10.1103/PhysRevLett.79.945

[33] Aumayr F., Burgdorfer J., Varga P., Winter H.P. Sputtering of insulator surfaces by slow highly charged ions: Coulomb explosion or defect mediated desorption?. Comm. At. Mol. Phys. 1999;(34):201.

[34] Hayderer G., Schmid M., Varga P., et al. Threshold for potential sputtering of LiF. Phys. Rev. Lett. 1999;(83):3948. DOI: 10.1103/PhysRevLett.83.3948

[35] Green T.A., Loubriel G.M., Richards P.M., et al. Time dependence of desorbed ground-state lithium atoms following pulsed-electron-beam irradiation of lithium fluoride. Phys. Rev. 1987;(35):781. DOI: 10.1103/PhysRevB.35.781

[36] Walkup R.E., Avouris P., Ghosh A. Positive-ion production by electron bombardment of alkali halides. Phys. Rev. B. 1987;(36):4577. DOI: 10.1103/PhysRevB.36.4577

[37] Szymonski M., Poradisz A., Czuba P., et al. Electron stimulated desorption of neutral species from (1 0 0) KCl surfaces. Surf. Sci. 1992;(260):295. DOI: 10.1016/0039-6028(92)90044-ZnO